A Large-Offset 2-D Seismic Survey for Imaging Imbricate Structures in Thrust Belts

Oz Yilmaz and Jie Zhang, GeoTomo LLC, Houston, Texas; and Alaattin Pince, Ahmet Aytunur, Aziz Elibuyuk, Serdar Uygun, Taner Onaran, and Ahmet Faruk Oner, Turkish Petroleum Corp., Ankara, Turkey*

Summary

Turkish Petroleum Corp. conducted a multichannel large-offset 2-D seismic survey near the town of Ergani, Southeast Turkey, in October, 2004. The objective is to image the complex, imbricate target structures in the Southeast Thrust Belt. The data were acquired using a common-spread recording geometry whereby the receiver spread was fixed for all shots. A total of 960 receiver groups was placed along a 23,975-m line traverse in the NNW-SSE dominant structural dip direction at a 25-m interval. A total of 145 shots was fired at a 250-m interval along the line traverse, beginning at a location outside the spread and 6 km away from the first receiver group in the SSE end of the line. The distance between the first and last shot locations is 35,975 m.

Land seismic data acquisition with conventional spread length (3,000 m) and conventional processing in midpoint-offset coordinates may fail to image complex imbricate structures associated with overthrust tectonics. Irregular topography associated with a rugged terrain, complexity of the near-surface that includes high-velocity layers and outcrops with significant lateral velocity variations, complexity of the overburden caused by allocthonous rocks, and the complexity of the target imbricate structures themselves, all pose challenges to exploration in thrust belts. The shot-domain analysis of the data from the large-offset Ergani seismic survey based on common-spread recording geometry, on the other hand, has indeed unraveled the imbricate structures that can lead to significant discoveries in the Southeast Thrust Belt.

We analyzed the Ergani large-offset data for earth modeling and imaging in depth. By a nonlinear first-arrival traveltime tomography, a velocity-depth model was estimated for the near-surface. Then, a subsurface velocity-depth model was estimated based on rms velocities derived from prestack time migration of shot gathers. Finally, prestack depth migration of shot gathers from a floating datum that is a close representation of the topography was performed to generate the subsurface image in depth.

Introduction

Shown in Figure 1 is a portion of one of the shot gathers from the Ergani large-offset line. Note that at small offsets the field record is overwhelmed by Rayleigh waves (ground roll) with backscattering, and essentially is void of reflection energy. When the same field record is examined at far offsets beyond the conventional spread length, note the abundance of supercritical reflections at large offsets. These reflections have been known to early researchers in exploration seismology (Richards, 1960).

In the common-spread recording geometry, the receiver spread is fixed for all shots (Figure 2). This has reduced the time in the field, significantly. The receiver spread comprises 960 groups, placed along a 23,975-m line traverse in the dominant structural dip direction (NNW-SSE) at 25-m intervals.

Of the 145 shot records acquired, we decided to use 94 shot gathers that are within the receiver spread in the final analysis. The maximum offset associated with these shot gathers is the same as the receiver spread length (23,975 m).

Data Analysis

Starting with the field records, we picked first-arrival times and edited traces. The maximum reciprocal error associated with the picked times is less than 15 ms, and the reciprocal errors for most of the shots are less than 10 ms. By using a nonlinear traveltime tomography (Zhang and Toksoz, 1998), we estimated a near-surface velocity-depth model that exhibits lateral and vertical velocity variations. The nonlinear tomography solution is based on not just the first-arrival times, which may include wave types other than refraction, but also changes in traveltime gradient. As such, within the near-surface, we were able to resolve strong lateral velocity variations associated with high-velocity outcrops. In deriving a final model for the near-surface, the traveltime tomography is iterated until the difference between the modeled and the actual traveltimes, measured as the rms error in inversion, has been reduced to a sufficiently small value comparable to the reciprocal traveltime errors. For quality control, we examined the raypaths associated with the near-surface model and made sure that they do not hit the bottom of the model. Also, we made sure that the match between the modeled traveltimes associated with the tomography solution for the near-surface and the observed (picked) traveltimes is satisfactory. From the near-surface model, we picked a floating datum that is a smoothed form of the topography along the line and the intermediate datum that defines the interface between the near-surface and the subsurface. Also, we defined a replacement velocity taken as the lateral average of the velocities along the intermediate datum. Finally, using all the relevant information about the near-surface velocity-depth model, we computed the shot and receiver statics. We also calculated shot and receiver

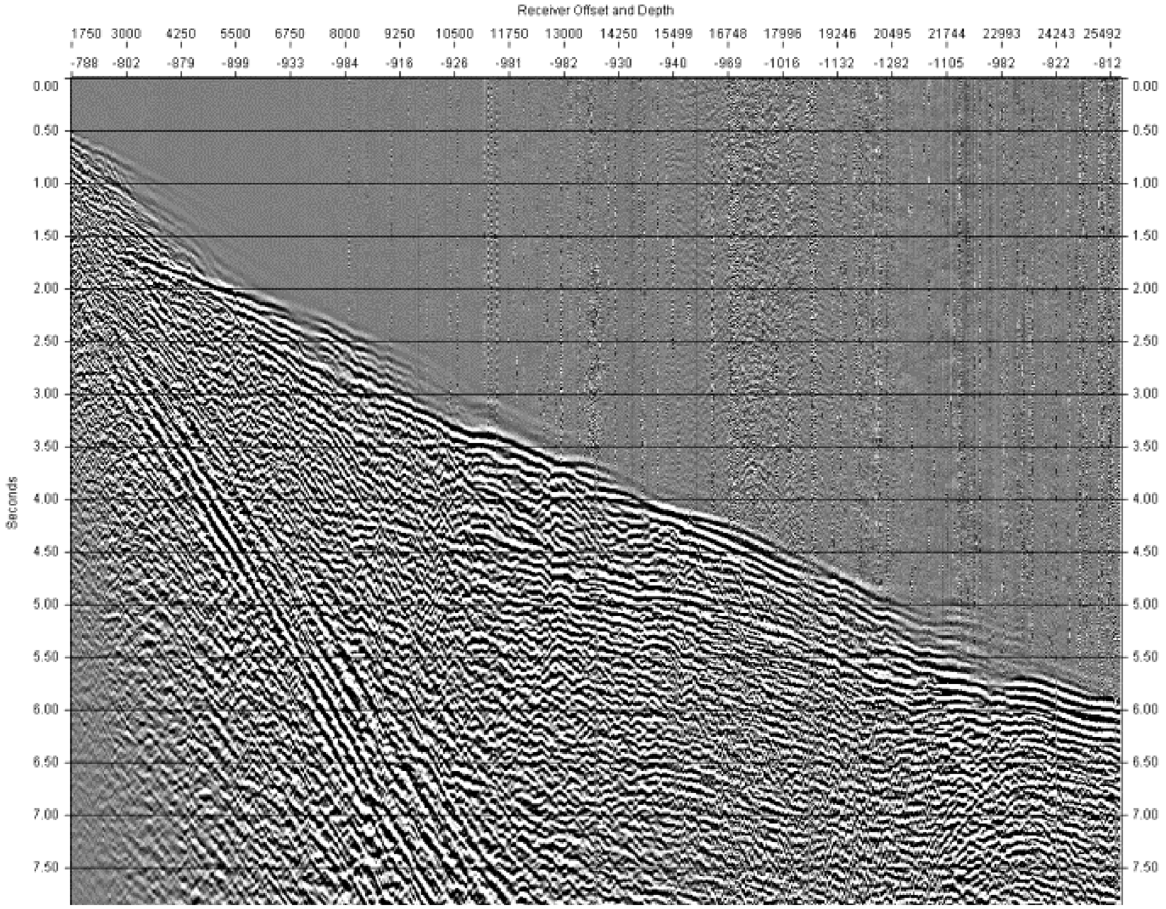

Figure 1. A portion of a field record from the large-offset Ergani line with offset range 1,750-25,500 m. Note the abundance of reflections at large offsets and the predominance of the ground-roll energy at near offsets.

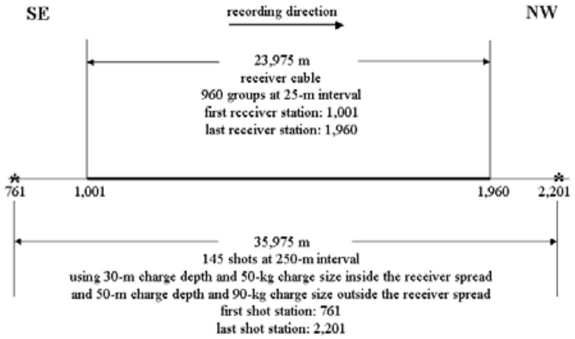

Figure 2. Common-spread recording geometry for the large-offset Ergani line.

residual statics based on the first-arrival times. Nevertheless, the residuals turned out to be rather small.

From the average amplitude spectra of selected shot records, we observed that the reflection signal at large offsets is within a bandwidth of 6-30 Hz. We applied a parsimonious signal processing sequence to the shot records that include (a) inside mute to eliminate the surface waves with large amplitudes, (b) outside mute to remove ambient noise before the first arrivals, and (c) time-variant spectral whitening to account for the nonstationarity of the signal and to flatten the spectrum within the signal passband (6-30 Hz). Finally, we applied the near-surface corrections and placed all the shots and receivers to the floating datum.

Next, we performed prestack time migration of shot gathers from the floating datum using a range of constant velocities and summed the individual images from all the shot gathers to obtain a set of multiple images of the subsurface. By combining these constant-velocity image panels, we created a velocity cube (Shurtleff, 1984), which we then interpreted in the next step to derive an rms velocity field associated with events in their migrated positions. This rms velocity field is better suited for Dix conversion to derive an interval velocity field compared to Dix conversion of stacking or DMO velocities, which are associated with events in their unmigrated positions (Yilmaz, 2001).

We used all three cross-sections of the velocity cube for picking the rms velocities. These are the distance along the line traverse versus event time after migration for a given rms velocity --- the X-T plane, the rms velocity versus event time after migration for a specific location along the line traverse--- the V-T plane, and the rms velocity versus the distance along the line traverse for a specific time --- the V-X plane that represents a time slice from the velocity cube. While the X-T plane provides structural consistency, the V-X plane provides the lateral consistency in picking the velocity strands.

We then migrated all of the shot gathers, individually, from the floating datum with the rms velocity field derived from the interpretation of the velocity cube, and obtained the image from prestack time migration. Next, we unmigrated (demigrated) the resulting image using the same rms velocity field as for prestack time migration. The demigrated section is a representation of a zero-offset wavefield; as such, it is the appropriate input to poststack depth migration compared to the conventional stack, which is only an approximate representation of a zero-offset section.

To construct an earth model in depth, we performed Dix conversion of the rms velocities to derive an interval velocity field. We then performed poststack depth migration of the demigrated section using the interval velocity field, and overlaid the image from poststack depth migration and the interval velocity field to check for consistency of the earth image with the earth model. Next, we interpreted a set of depth horizons associated with layer boundaries with significant velocity contrast. We then divided each layer into a set of thin layers by creating phantom horizons so as to preserve the vertical and lateral velocity variations within each layer inferred by the interval velocity field, and applied lateral and vertical smoothing to velocities within each layer.

Finally, we performed depth migration of the shot gathers, individually, from the floating datum, and sorted the resulting shot images to common-receiver gathers in depth (one type of image gathers). To obtain the image from prestack depth migration, we simply stacked the traces in each common-receiver gather. Prestack depth migration based on migration of shot gathers (Schultz and Sherwood, 1980; Reshef and Kosloff, 1986) was performed using the phase-shift-plus-interpolation (PSPI) algorithm (Gazdag and Squazzerro, 1984), adapted to start the imaging from a floating datum (Reshef, 1991).

Comparison with Conventional Seismic Data

Figure 3 shows the image from poststack time migration of the data from the CMP line recorded with conventional spread length (less than 3,000 m) along the same line traverse as that of the large-offset seismic line. The data analysis was done using a conventional processing workflow. Note the absence of any coherent signal in this section. It would not matter if the imaging was performed before or after stack, in time or in depth --- the primary cause of this poor image is that the shot records from the vintage CMP line contain weak reflection signal overwhelmed by strong surface waves within the conventional spread length that corresponds to the subcritical region of wave propagation. In contrast, in prestack migration of the data from the large-offset line, we made use of the supercritical reflections recorded at large offsets. Another major difference in the data analysis of the two seismic lines is that we migrated the large-offset data from a floating datum, not from a flat datum as in the case of the conventional data.

Conclusions

The Ergani large-offset land seismic survey has indeed provided immensely valuable information for the delineation of target imbricate structures associated with overthrust tectonics in the Southeast Thrust Belt of Turkey. The images from prestack time and depth migrations clearly exhibit structural features that have not been previously observed in the seismic sections derived from conventional surveys with spread lengths less than 3,000 m.

Acknowledgements

We are grateful to the Exploration Division of the Turkish Petroleum for conducting this project and for granting the permission to publish the results.

References

Gazdag, J. and Squazerro, P., 1984, Migration of seismic data by phase-shift plus interpolation: Geophysics, **49**, 124-131.

Reshef, M., 1991, Migration from irregular topography: Geophysics, 50, 1333-1335.
Reshef, M. and Kosloff, D., 1986, Migration of common-shot gathers: Geophysics, **51**, 324-331.

Richards, T. C., 1960, Wide-angle reflections and their application to finding limestone structures in the Foothills of Western Canada: Geophysics, **25**, 385-407.

Schultz, P. S. and Sherwood, J. W. C., 1980, Depth migration before stack: Geophysics, **45**, 361-375.

Shurtleff, R., 1984, An *F-K* procedure for prestack migration and velocity analysis: Presented at the 46th Ann. Mtg. European Asn. Expl. Geophys.

Yilmaz, O., 2001, Seismic Data Analysis: Society of Exploration Geophysicists, Tulsa.

Zhang, J. and Toksoz, M. N., 1998, Nonlinear refraction traveltime tomography: Geophysics, **63**, 1726-1737.

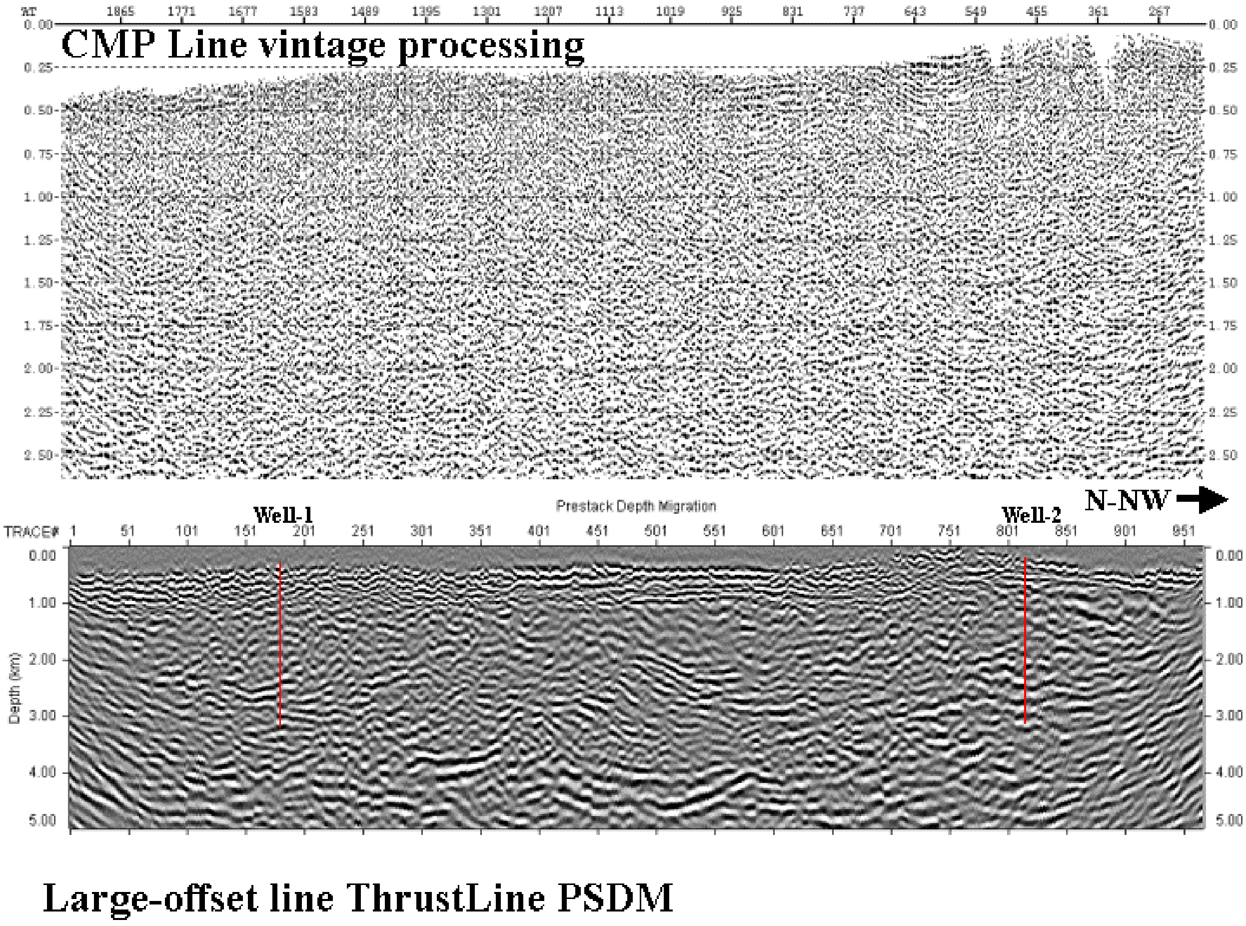

Figure 3. Top: Poststack time migration of the data from the CMP line recorded with conventional spread length (less than 3,000 m) along the same line traverse as the large-offset seismic line. The data analysis was done using a conventional processing workflow. Bottom: Prestack depth migration of the large-offset data from the workflow described in this paper. The length of this section spans the full extent of the receiver spread (24 km) down to 5 km. The section is posted with respect to a seismic reference datum of –1,300 m. A 6-30 Hz bandpass filter has been applied to both sections.

EDITED REFERENCES

Note: This reference list is a copy-edited version of the reference list submitted by the author. Reference lists for the 2005 SEG Technical Program Expanded Abstracts have been copy edited so that references provided with the online metadata for each paper will achieve a high degree of linking to cited sources that appear on the Web.

A Large-Offset 2-D Seismic Survey for Imaging Imbricate Structures in Thrust Belts

References

Gazdag, J. and P. Squazerro, 1984, Migration of seismic data by phase-shift plus interpolation: Geophysics, **49**, 124–131.

Reshef, M., 1991, Migration from irregular topography: Geophysics, **50**, 1333–1335.

Reshef, M., and D. Kosloff, 1986, Migration of commonshot gathers: Geophysics, **51**, 324–331.

Richards, T. C., 1960, Wide-angle reflections and their application to finding limestone structures in the Foothills of Western Canada: Geophysics, **25**, 385–407.

Schultz, P. S., and J. W. C. Sherwood, 1980, Depth migration before stack: Geophysics, **45**, 361–375.

Shurtleff, R., 1984, An *F-K* procedure for prestack migration and velocity analysis: Presented at the 46th Annual International Meeting, EAGE.

Yilmaz, O., 2001, Seismic data analysis: SEG.

Zhang, J., and M. N. Toksöz, 1998, Nonlinear refraction traveltime tomography: Geophysics, **63**, 1726–1737.